HAL open science

Drought recorded by Ba/Ca in coastal benthic foraminifera

Inda Brinkmann, Christine Barras, Tom Jilbert, Tomas Næraa, K. Mareike Paul, Magali Schweizer, Helena L. Filipsson

▶ **To cite this version:**

Inda Brinkmann, Christine Barras, Tom Jilbert, Tomas Næraa, K. Mareike Paul, et al.. Drought recorded by Ba/Ca in coastal benthic foraminifera. Biogeosciences, 2022, 19, pp.2523-2535. 10.5194/bg-19-2523-2022 . insu-03682338

HAL Id: insu-03682338

https://insu.hal.science/insu-03682338v1

Submitted on 31 May 2022

HAL is a multi-disciplinary open access archive for the deposit and dissemination of scientific research documents, whether they are published or not. The documents may come from teaching and research institutions in France or abroad, or from public or private research centers.

L'archive ouverte pluridisciplinaire **HAL**, est destinée au dépôt et à la diffusion de documents scientifiques de niveau recherche, publiés ou non, émanant des établissements d'enseignement et de recherche français ou étrangers, des laboratoires publics ou privés.

Distributed under a Creative Commons Attribution 4.0 International License

Biogeosciences, 19, 2523–2535, 2022
https://doi.org/10.5194/bg-19-2523-2022
© Author(s) 2022. This work is distributed under
the Creative Commons Attribution 4.0 License.

Biogeosciences
Open Access
EGU

Research article

Drought recorded by Ba/Ca in coastal benthic foraminifera

Inda Brinkmann[1], Christine Barras[2], Tom Jilbert[3], Tomas Næraa[1], K. Mareike Paul[3], Magali Schweizer[2], and Helena L. Filipsson[1]

[1]Department of Geology, Lund University, Sölvegatan 12, 223 62 Lund, Sweden
[2]LPG UMR 6112, University of Angers, Nantes Université, Le Mans Université, CNRS, 2 bd Lavoisier 49045, Angers CEDEX 01, France
[3]Department of Geosciences and Geography, Faculty of Science, University of Helsinki, Gustaf Hällström katu 2, 00560 Helsinki, Finland

Correspondence: Inda Brinkmann (inda.brinkmann@geol.lu.se)

Received: 17 November 2021 – Discussion started: 25 November 2021
Revised: 21 March 2022 – Accepted: 25 March 2022 – Published: 16 May 2022

Abstract. Increasing occurrences of extreme weather events, such as the 2018 drought over northern Europe, are a concerning issue under global climate change. High-resolution archives of natural hydroclimate proxies, such as rapidly accumulating sediments containing biogenic carbonates, offer the potential to investigate the frequency and mechanisms of such events in the past. Droughts alter the barium (Ba) concentration of near-continent seawater through the reduction in Ba input from terrestrial runoff, which in turn may be recorded as changes in the chemical composition (Ba/Ca) of foraminiferal calcium carbonates accumulating in sediments. However, so far the use of Ba/Ca as a discharge indicator has been restricted to planktonic foraminifera, despite the high relative abundance of benthic species in coastal, shallow-water sites. Moreover, benthic foraminiferal Ba/Ca has mainly been used in open-ocean records as a proxy for paleo-productivity. Here we report on a new geochemical data set measured from living (CTG-labeled) benthic foraminiferal species to investigate the capability of benthic Ba/Ca to record changes in river runoff over a gradient of contrasting hydroclimatic conditions. Individual foraminifera (*Bulimina marginata*, *Nonionellina labradorica*) were analyzed by laser-ablation ICP-MS over a seasonal and spatial gradient within Gullmar Fjord, Swedish west coast, during 2018–2019. The results are compared to an extensive meteorological and hydrological data set, as well as sediment and pore-water geochemistry. Benthic foraminiferal Ba/Ca correlates significantly to riverine runoff; however, the signals contain both spatial trends with distance to Ba source and species-specific influences such as micro-habitat preferences. We deduce that shallow-infaunal foraminifera are especially suitable as proxy for terrestrial Ba input and discuss the potential influence of water-column and pore-water Ba cycling. While distance to Ba source, water depth, pore-water geochemistry, and species-specific effects need to be considered in interpreting the data, our results demonstrate confidence in the use of Ba/Ca of benthic foraminifera from near-continent records as a proxy for past riverine discharge and to identify periods of drought.

1 Introduction

Extreme weather events, such as drought and heat waves, have a devastating impact globally (e.g., Sternberg, 2011). Droughts occur through an interplay of below-average precipitation, high evapotranspiration, and hydrological preconditions, such as soil moisture and water storage capacity (e.g., Tallaksen and Van Lanen, 2004). Alone in the 21st century, Europe was affected by a series of exceptionally severe drought events (e.g., Bastos et al., 2020a). With anthropogenic global warming accelerating the internal processes driving hydroclimate variability, droughts are expected to keep increasing in frequency and severeness in the future (e.g., Cook et al., 2020). Thus, it is imperative to document droughts pre-dating anthropogenically forced climate change to define a baseline of natural hydroclimatic variability.

Hydrological drought, defined as deficiency in water supply including below-normal river discharge, is one of the main comprehensive indicators for accumulated hydrological responses to a reduction in precipitation on a wide spatial and temporal scale (e.g., Tallaksen and Van Lanen, 2004). A range of natural archives for historical droughts exist in the terrestrial environment, including dendrochronological, ice-core- and speleothem-based proxy records (e.g., Steiger et al., 2018). In aquatic systems, sediments offer the potential to record hydrological conditions on land through changing fluxes of materials across the land–water interface. One potential sediment proxy capable of quantifying hydrological drought is the barium to calcium ratio (Ba/Ca) in biogenic carbonates formed in the coastal marine environment. Barium in seawater is dominantly sourced from fluvial input (e.g., Wolgemuth and Broecker, 1970) and proportionally incorporated in biogenic calcium carbonates as a substitute for the Ca^{2+} ion (e.g., de Nooijer et al., 2017). Hence, changes in fluvial Ba inputs may be expected to influence carbonate Ba/Ca in the nearshore environment.

While Ba/Ca is applied for paleoclimatic reconstructions, the focus so far has been on corals in tropical environments (e.g., Saha et al., 2018) and planktonic foraminifera (e.g., Bahr et al., 2013; Mojtahid et al., 2019). Moreover, Ba/Ca of benthic foraminifera is dominantly interpreted as a paleoproductivity proxy (e.g., Mojtahid et al., 2019; Ní Fhlaithearta et al., 2010), due to the nutrient-like cycling of Ba in seawater (e.g., Dehairs et al., 1980; Paytan and Griffith, 2007). Benthic foraminifera are ubiquitous in coastal sediments, and concurrently coastal sediment records are important paleoclimate archives due to their high temporal resolution and transitional position between the terrestrial and marine realm (review by Howe et al., 2010; Murray, 2006). While rare applications of benthic foraminiferal Ba/Ca as a runoff indicator exist (Groeneveld et al., 2018; Ni et al., 2020), studies focusing on living benthic foraminifera are distinctly lacking. In situ, core-top approaches with living foraminifera are, however, essential to calibrate a proxy and create a reliable baseline of empirical observations by correcting for species-specific biases and seasonal-scale mechanisms influencing Ba/Ca in a coastal environment.

The drought and heat wave of 2018 that affected northern and central Europe, including Scandinavia, was exceptional in its severeness (e.g., Peters et al., 2020), and was followed by a warm and wet year in 2019 (Swedish Meteorological and Hydrological Institute, SMHI). This contrast in precipitation between 2018 and 2019 presents a unique opportunity to study the response of benthic foraminiferal trace-elemental concentrations to changes in riverine discharge. Here we test the hypothesis of benthic foraminiferal Ba/Ca as a tracer for riverine discharge, assess the potential of identifying drought events in sediment foraminiferal records, and evaluate the broader implications for the interpretation of benthic Ba/Ca in paleo-studies in coastal environments.

2 Site description: Gullmar Fjord, Swedish west coast

Gullmar Fjord (GF; ca. 28 km by 1–2 km; Fig. 1) has a maximum water depth of 120 m, located centrally at Alsbäck, and a sill depth of 43 m towards the Skagerrak. The sediments in the fjord's deep basin are comprised of silty clays with a low sand content and an organic carbon content of approximately 3 % in surface sediments (e.g., Gustafsson and Nordberg, 2001). Phytoplankton blooms occur typically biannually in spring and autumn (dominated by diatoms and dinoflagellates, respectively; e.g., Gustafsson and Nordberg, 2001).

The river Örekilsälven is the main contributor of freshwater to the fjord (annual average discharge of $24\,m^3\,s^{-1}$ vs. $0.6–1.0\,m^3\,s^{-1}$ inflow from catchment north and south of GF) and represents > 80 % of the fjord's catchment area ($1338\,km^2$ out of $\sim 1600\,km^2$; Fig. 1). The annual and seasonal discharge is proportional to the respective hinterland precipitation. Örekilsälven's inflow contributes to the fjord's brackish surface water layer (∼ 0.5 m; Fig. 1).

Further, the fjord's hydrography is governed by the water exchange with Skagerrak (North Sea) and Kattegat (Baltic) (e.g., Arneborg, 2004). While water masses exchange more readily above sill level with Kattegat waters, the deep basin (> 50 m) flushes approximately annually, typically between January and April, and these ventilation events are driven by wind direction and the winter NAO pattern (e.g., Filipsson and Nordberg, 2004). Except for periods of water renewals, the fjord's waters are stratified in layers of distinct salinity and renewal times (e.g., Arneborg, 2004; compare Fig. 1).

3 Material and methods

3.1 Sampling

Our study is based on three seasonal sampling campaigns (September 2018, February and June 2019) in Gullmar Fjord, Swedish west coast (Table 1). During each campaign two sites were sampled, GF 71 (water depth ∼ 70 m b.s.l.) and GF 117 (∼ 116 m b.s.l.). A CTD with O_2-probe and Niskin water-collection system was deployed to record temperature, dissolved oxygen concentration ($[O_2]$), and salinity (reported using the practical salinity scale) throughout the water column and to collect bottom water. Bottom water was sampled in bottles of 25–40 mL and refrigerated until further analyses. Sediment cores were collected with a GEMAX® twin-barrel corer (modified Gemini corer, 9 cm diameter, from Oy Kart AB, Finland) in two casts. For foraminiferal analyses, the top 1 cm of two duplicate cores from the first casts was sliced in 0.5 cm sections (ca. 32 mL sediment; 0–0.5, 0.5–1.0 cm). Each sample was placed into an HDPE (high-density polyethylene) bottle with roughly equal amounts of ambient bottom water and 36 µL of CellTracker™ Green (CTG) CMFDA dye (5-chloromethylfluorescein diacetate; with dimethyl sulfoxide (DMSO); both ThermoFisher Scien-

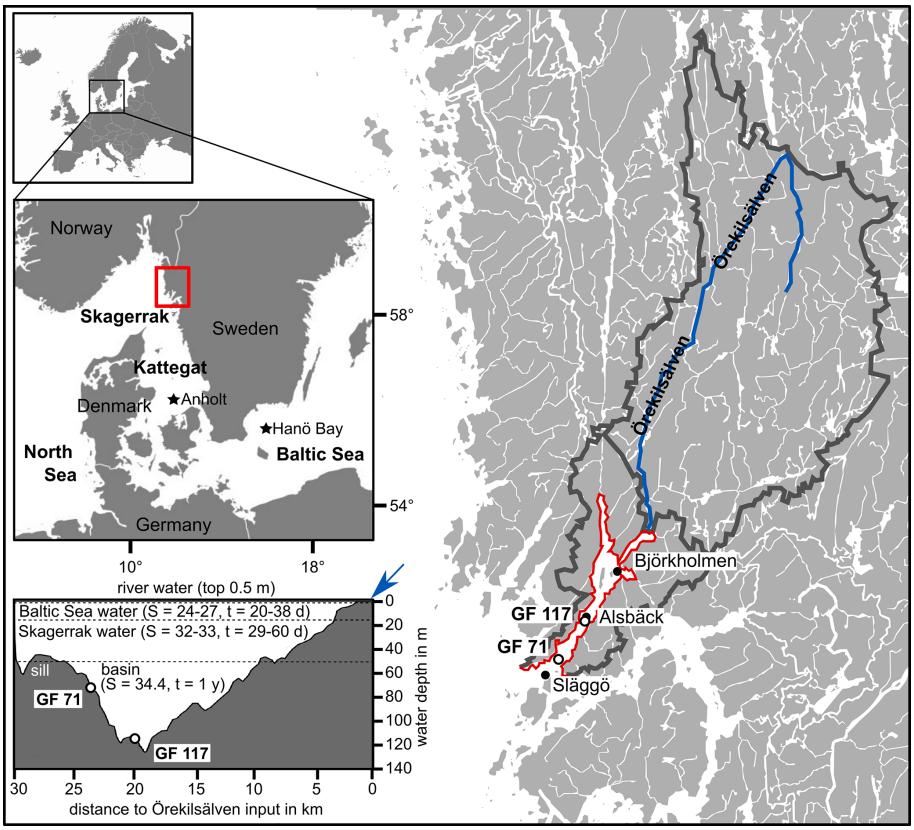

Figure 1. Location of the study area within Europe and on the west coast of Sweden (marked by red rectangle) giving an overview of Gullmar Fjord and Örekilsälven, including cumulative catchment area (outlined in dark grey). The study sites GF 71 and GF 117, and environmental monitoring sites Alsbäck, Björkholmen, and Släggö are indicated. A transect of Gullmar Fjord with water masses of different sources is given (S = salinity, t = typical residence time in days (d) or years (yr); after Arneborg, 2004), with indication of Örekilsälven input (blue arrow). Maps modified after SMHI and Groeneveld et al. (2018).

tific) to reach a final CTG concentration of 1 µM. The samples were incubated at 6 °C (in situ bottom-water temperature 6.5–7.1 °C) for 10 h for living cells to take up the CTG epifluorescent tracer for later observation (e.g., Bernhard et al., 2006), and thereafter preserved in 40 mL of ethanol.

At site GF 117, one set of duplicate cores was sampled for bottom-, pore-water, and solid-phase geochemical analyses. During each campaign, the first core was used for bottom-water and pore-water sampling using Rhizons™ at 2 cm vertical resolution. The samples were collected into 10 mL polyethylene syringes through pre-drilled holes (diameter 4 mm; e.g., Jokinen et al., 2020) immediately after core retrieval. Within a few hours after retrieval, all water samples were transferred into 15 mL polypropylene centrifuge tubes and acidified to 1 M HNO_3 for elemental analyses.

The second core from each pair was sampled for solid-phase parameters. In September 2018, the second core was immediately sampled on deck after core retrieval. In February and June 2019, the second core was sampled a few hours after core retrieval inside a cool room. Each core was sliced at 1 cm intervals (0–10 cm) and 2 cm intervals (10–30 cm). Each sediment slice was transferred into plastic bags, which were carefully sealed under water, and transferred into gas-tight glass jars. The jars were flushed with N_2 and stored in the dark at 4 °C prior to further processing to avoid oxidation of the samples. In preparation for solid-phases analyses, each wet sediment slice was subsampled inside a N_2-flushed glove bag and frozen for 24 h at −20 °C. Subsequently, each sample was freeze-dried for 48 h, homogenized, and weighed in between each step to determine the water [g] and salt contents [g], and porosity [$cm^3\,cm^{-3}$] using the bottom-water salinity and the assumed solid-phase density of 2.65 $g\,cm^{-3}$ (Burdige, 2006). The water and salt contents were used to determine the salt-free weight of the dry sediment, which is needed to correct the solid-phase elemental concentrations for salt dilution.

3.2 Geochemical analyses of benthic foraminifera

Living (CTG-labeled) specimens of *Bulimina marginata* d'Orbigny, 1826 and *Nonionellina labradorica* (Dawson, 1960) were selected for laser-ablation (LA) ICP-MS trace element analysis, according to their availability in each sam-

Table 1. Sampling sites and number of analyzed specimens per species and sediment interval for each site and sampling occasion, before and after quality control of measurements. Median Ba/Ca with median average deviation (MAD) of n-chambers in µmol mol^{-1} per species, site, and season (number of data points, i.e., analyzed specimens, indicated in brackets) for top 1 cm sediment.

Site (water depth) position	Species	Sampling date	Number of analyzed specimens		After quality control (n-chamber spots)		Median Ba/Ca with MAD (µmol mol^{-1})
			0–0.5 cm	0.5–1.0 cm	0–0.5 cm	0.5–1.0 cm	0–1 cm
GF 117 inner fjord (115–117 m)	*N. labradorica*	17 September 2018	9*	11	8	9	2.77 ± 1.13 (17)
		24 February 2019	10	8	8	7	3.43 ± 1.53 (15)
		11 June 2019	7	9	7	6	2.89 ± 0.71 (13)
58°19.695′ N, 11°33.147′ E	*B. marginata*	17 September 2018	17*	10	15	9	1.82 ± 1.04 (24)
		24 February 2019	9	8	4	5	6.84 ± 1.98 (9)
		11 June 2019	11	10	10	10	6.63 ± 2.25 (20)
GF 71 outer fjord (69–71 m)	*N. labradorica*	17 September 2018	10	10	9	9	1.97 ± 0.26 (18)
		24 February 2019	10	10	8	10	4.33 ± 1.07 (18)
		11 June 2019	11	11	10	11	4.10 ± 0.72 (21)
58°17.116′ N, 11°30.546′ E	*B. marginata*	17 September 2018	13	10	4	8	0.55 ± 0.13 (12)
		24 February 2019	11	11	8	7	2.82 ± 1.09 (15)
		11 June 2019	10	11	8	9	2.19 ± 1.15 (17)

* marks samples compiled from two duplicate cores.

ple (i.e., abundance). To extract specimens the samples were washed over a set of sieves (63, 100 µm) and the > 100 µm fraction was wet-picked under epifluorescent light (Nikon SMZ 1500 with Nikon Intensilight C-HGFI). When a single core produced an insufficient number of specimens for analyses, specimens from the duplicate cores were also analyzed. An average of 10 living specimens – identified by their CTG-label – per sediment interval and site were selected for geochemical analyses (Table 1). The tests were treated with NaOCl (5 %) for 2–5 h to remove organic materials including cytoplasm (e.g., Mashiotta et al., 1999), following a triple rinse with Milli-Q (Milli-Q Integral, EMD Millipore Corporation, Billerica, MA, USA) water and dried at room temperature.

Laser ablation ICP-MS analyses were carried out at the Department of Geology, Lund University, Sweden, using a Bruker Aurora Elite (quadrupole) ICP-MS and a 193 nm Cetac Analyte G2 excimer laser installed with a two-volume HelEx2 sample cell. Helium was used as carrier gas (approximately 0.8 L min^{-1}) in combination with a down-stream addition of argon (approximately 0.95 L min^{-1}) after the sample chamber. The counts of the isotope masses ^{138}Ba, as well as ^{27}Al, ^{43}Ca, ^{55}Mn and ^{66}Zn, were acquired at 5 Hz (i.e., laser shots per second). To obtain a stable isotope signal a "squid" was inserted downstream of the sample chamber. The scan time of the ICP-MS was synchronized with the laser repetition rate to minimize artificial fluctuations of the isotope signals. Spot sizes were adapted to chamber sizes of the investigated species (75 × 75, 55 × 75, 50 × 70 µm) but kept constant within individual sessions and applied to both samples and standard material. Previous studies indicate that using variable spot sizes does not influence elemental fractionation during LA measurements on foraminiferal tests (e.g., Eggins et al., 1998). The samples were analyzed at an energy density of 1 J cm^{-2} to avoid breaking of foraminiferal tests and to obtain a longer ablation signal. The conditions were mimicked for the secondary carbonate standards. Glass standards, US National Institute of Standards and Technology SRM NIST610 and 612 (see below), were analyzed at 3 J cm^{-2} for optimized ablation efficiency. The LA ICP-MS was operated in manual mode for sample analyses. Elemental baseline levels before each spot analysis were measured for at least 30 s.

NIST610 was used for instrument tuning to ascertain high and stable signal counts on the studied elements, low oxide production (< 0.5 % monitoring ^{238}U / ^{238}U^{16}O and ^{232}Th / ^{232}Th^{16}O), and low elemental fractionation (^{232}Th / ^{238}U ratios close to 1). NIST610 was used as external calibration material with GeoReM (Geological and Environmental Reference Materials, 2021; Jochum et al., 2005) composition values (via http://georem.mpch-mainz.gwdg.de, last access: 30 April 2021), giving an average internal relative precision for Ba of 4.4 % (based on the relative standard deviation of raw data (cps) per analysis session; Table S1), and to correct for instrumental drift. Primary standard NIST610 and secondary standards, NIST612, MACS-3 (MicroAnalytical Carbonate Standard, United States Geological Survey, 2012; Jochum et al., 2012), and JCt-1 and JCp-1 (AIST Japan calcium carbonate pellets), were run at the beginning and end of each session and the data used to monitor the quality of the analyses (Table S1). A selection

of these – NIST610, MACS-3, JCp-1 – were additionally run after each 10–15 sample spots.

For each specimen, the final (n), penultimate ($n-1$), and antepenultimate ($n-2$) chambers (as far as possible) were targeted and ablated from the outside to inside of the wall. For *B. marginata* also the signal of the initial chambers was measured with a laser-spot covering proloculus and following chambers and ablating through these chambers (referred to as "p"). We consider this to represent a bulk signal of an extended growth period, including the primary signal of the juvenile chambers as well subsequently added layers of calcite with each new chamber addition (e.g., Erez, 2003).

3.3 Benthic foraminiferal trace-element data processing

Raw counts were converted to elemental concentrations (ppm) with the software package Igor Pro 6.37 with Iolite v3.5 (Paton et al., 2011). The element ratios were calculated based on the average concentration measured during the ablation period of the primary test calcium carbonate. This signal interval was determined through manual examination of each trace element profile. Constant counts of ^{43}Ca were used to find integration intervals of calcite ablation. Intervals of enriched signals of ^{27}Al, ^{55}Mn, and/or ^{66}Zn, indicative of secondary surface coatings and/or contaminations, were excluded. Such were typically measured at the beginning and/or end of each profile (corresponding to the outer and inner test wall surfaces, respectively), with relatively constant raw elemental counts intermediate (see also e.g., Ni et al., 2020). Trace elemental ratios (TE/Ca) were calculated with the assumption of the TEs being bound as carbonate (assuming 40 % wt Ca in the $CaCO_3$ matrix) and normalized to calcium.

In total, 486 ablation profiles (> 15 data points of the ICP-MS per signal) were performed on chambers (n, $n-1$, $n-2$ and p) of *B. marginata* and 346 on chambers (n, $n-1$, $n-2$) of *N. labradorica* specimens and evaluated according to the following criteria (i.e., quality control): (1) [Ba] higher than limit of quantification (LOQ = baseline signal $+ 10 \times \sigma$; σ = standard deviation of baseline signal) (9 signals), (2) exclusion of ablation signals with potential clay contamination (i.e., Al/Ca > 0.4 mmol mol^{-1}; Wit et al., 2010) (30 signals), (3) application of a 95 % confidence limit on Ba/Ca, for each species, site and season, to remove outliers (i.e., > 2× standard deviation) (39 signals). In total, 78 of 832 (9.4 %) ablation profiles were rejected from further analyses.

From the benthic foraminiferal Ba/Ca values the median and MAD were calculated per species, season, and site, to limit the influence of extreme outliers. As no systematic differences between sediment intervals were observed (Welch ANOVA, Table S2), Ba/Ca data were pooled. If not indicated otherwise, only data on n-chambers were considered, assuming these were precipitated in close temporal proximity to the time of sampling.

3.4 Pore-water and sediment trace-element analyses

The acidified bottom-water and pore-water samples were analyzed for elemental concentrations of Ba by inductively coupled plasma-mass spectrometry (ICP-MS; Thermo Scientific XSeries 2; Utrecht University, Department of Earth Sciences) and of manganese (Mn), iron (Fe), and sulfur (S) by inductively coupled plasma-optical emission spectrometry (ICP-OES; Thermo Scientific iCAP 6000; Helsinki University, Ecosystems and Environment Research Program). For the determination of total solid-phase Ba, Mn, and Fe concentrations, an aliquot of 100–125 mg of freeze-dried and powdered sediment was digested in 2.5 mL solution of 3 : 2 $HClO_4$ (70 %) and HNO_3 (65 %) and HF (40 %). The Teflon vessels were left with closed lids overnight under a fume hood with water trap on a hotplate at 90 °C. After 12 h, the lids were removed, and the extracts were heated to 140 °C to evaporate the acids. The evaporate was redissolved in 25 mL HNO_3 (4.5 %) and left overnight on a hotplate at 90 °C. The next day, the Teflon vessels were weighed again to determine the dilution of the final solutions. Subsequently, the sample residues were analyzed by ICP-MS (Ba) at Utrecht University and by ICP-OES (Mn, Fe) at the University of Helsinki. Based on sediment sample duplicates the average analytical uncertainties were 6 ppm (Ba), 3.5 ppm (Mn), and 18.6 ppm (Fe).

3.5 Meteorological and hydrological data

All meteorological, hydrographical, and hydrological data of the Swedish west coast, the sill fjord, and its catchment area are publicly available from SMHI (SMHI, 2021). We used the SHARK hydrographic database (https://sharkweb.smhi.se/hamta-data/, last access: 10 February 2021; SMHI, 2021) to obtain monthly data on salinity, [O_2], and/or chlorophyll *a* across 2018 and 2019 from three fjord stations Släggö (58°25.98′ N, 11°43.57′ E, 70 m b.s.l.), Alsbäck (58°19.40′ N, 11°32.80′ E, 120 m b.s.l.), and Björkholmen (58°23.26′ N, 11°37.60′ E, 50 m b.s.l.) (Fig. 1), of which Alsbäck is closely located to GF 117. Daily runoff and sediment load data were collected from the hydrological database "vattenweb" (https://www.smhi.se/data/hydrologi/vattenwebb, last access: 10 February 2021), partly based on the S-HYPE (Hydrological Predictions for the Environment) model maintained by SMHI. For both hydrological and meteorological data, the averages were calculated for 30, 60, 90, and 120 d periods preceding the sampling occasions directly or by 1 month, respectively (i.e., four periods ending on and four periods ending 1 month prior to the sampling dates).

3.6 Statistical analyses

All statistical analyses were performed with the software package PAST 4.05 (Hammer et al., 2001), considering a p value of < 0.05 as significant. Since parts of the data

were non-normally distributed (Shapiro–Wilk's test) and heteroscedastic (Bartlett's test), we performed ANOVA Welch or Kruskal–Wallis tests associated with Mann–Whitney post hoc tests to compare Ba/Ca between seasons, sediment intervals, species, and chambers (non-parametric tests). To determine strength and direction of monotonic relationships between categorial and continuous variables (e.g., chamber number and Ba/Ca) Spearman rank correlations were tested. We used Pearson's r to determine the relationship between two continuous variables (e.g., Ba/Ca and river discharge; dissolved TE concentrations), using normalized data if testing data across several sites and species (0–1 scaling).

4 Results and discussion

4.1 Contrasting hydroclimatic conditions in 2018/2019 and Ba/Ca shift in benthic foraminifera

In the year 2018 north-western Europe experienced severe heat and drought, ascribed to an interplaying Rossby Wave-7 circulation and positive North Atlantic Oscillation index (NAO) across the Northern Hemisphere (e.g., Kornhuber et al., 2019). The occurrence of this large-scale synoptic weather pattern has increased within the last three decades, being responsible also for the 2003, 2006, 2012, and 2015 drought events, in response to anthropogenic global warming (e.g., Kornhuber et al., 2019).

In Sweden, the drought was expressed as above-normal mean air temperatures and below-normal precipitation and distinctly imprinted in the seasonal runoff conditions across the country (Fig. 2a; SMHI).

While the hydrological cycle naturally experiences seasonal variability – high runoff in winter, spring, and autumn (150 mm each), low in summer (50 mm) – in 2018 already the spring was exceptionally dry. The very dry spring conditions likely contributed to amplifying the following summer drought (Bastos et al., 2020b), with summer and autumn precipitation being 50 %–75 % of the 1961–1990 average (southwestern Sweden).

On the contrary, the year 2019 registered above-average annual precipitation (120 %–130 % in southwestern Sweden), although strongly varying monthly (e.g., record-low in April, highest precipitation in May), and was warmer than average both in Sweden and globally (Dunn et al., 2020).

In the study area the contrasting hydroclimate conditions of 2018 and 2019 is expressed in annual average discharges of Örekilsälven to GF of 18.5 and 29.0 $m^3 s^{-1}$, respectively (Fig. 2). Coinciding, the benthic foraminiferal Ba/Ca shifted significantly in most samples, corresponding to an increase of up to 5 times (Table 1; Figs. 2b, 3, S1).

Correlations of foraminiferal Ba/Ca with the shift in hydroclimatic conditions of the consecutive years imply Ba/Ca representing the discharge 60–90 d prior to sampling ($r =$ 0.36–0.40) or discharge conditions preceding the Ba/Ca record by 1 month ($r = 0.46$–0.48; testing Ba/Ca across species and sites; Table S3). On the one hand, a potential lag time in the transport of riverine Ba to coastal sediments is conceivable, determined by marine processes influencing the sinking and deposition of Ba. This may be influenced by environmental conditions including the degree of primary productivity and/or bottom-water oxygenation state and thus temporally variable (further discussed in Sect. 4.2). On the other hand, the lagging aims to account for the uncertainties in the exact timing of foraminiferal growth. In this respect, the lag is probably most applicable to the foraminiferal samples collected in February 2019, assuming the majority of foraminiferal calcite was precipitated in connection to the preceding autumn phytoplankton bloom (e.g., Gustafsson and Nordberg, 2001; Fig. S2). Temporal differences in reproduction and growth of the species could explain the differing strength of correlation to the observed hydroclimatic conditions, as well as species-specific intrinsic factors that can influence benthic foraminiferal Ba/Ca (further discussed in Sect. 4.3). While riverine Ba concentrations may also be temporally variable and thus could conceivably affect foraminiferal Ba/Ca signals, we consider such variations negligible in comparison to the contrasting Ba supply in response to the hydrological conditions of 2018 and 2019.

The range of Ba/Ca across 2018/19 varies between the inner-fjord and the outer-fjord site in all species (1–4 times vs. 2–5 times, respectively). The Ba/Ca signal of the outer-fjord site is generally lower than in the inner fjord in *B. marginata*, although the same is not resolved by *N. labradorica* (Fig. 3). To explain the trend in *B. marginata*, we hypothesize that the outer-fjord site experiences larger differences between periods of contrasting influence of Ba-rich river water versus low-Ba seawater of Kattegat and Skagerrak. This is plausible as the influence of Ba addition by Örekilsälven discharge diminishes, and the frequency of water exchange events increases, from the inner to outer fjord (Fig. S3). The fjord topography could be an additional factor, with the deep basin acting as a Ba sink. While the effects are minor compared to those of prolonged drought periods, these spatial factors should be of consideration when inferring hydroclimatic gradients from foraminiferal Ba/Ca.

The Ba/Ca signals of 2018 compared well to values expected for environments with negligible terrestrial influence (e.g., Anholt site in Kattegat; see Fig. 1, compilation of data from this study and Groeneveld et al., 2018 in Fig. 3); thus they are anomalously low considering the close spatial proximity to a river mouth (< 25 km; Fig. 1) and seasonally restricted water exchanges with the open sea (Fig. S3). On the other hand, Ba/Ca of the 2019 fjord samples ranges distinctly higher, consistent with the expectation for coastal environments such as the Baltic Sea (Fig. 1 for location; Fig. 3).

We deduce that the drought prevailing in spring and summer 2018 caused a distinct lack of riverine input, interrupting terrestrial Ba addition to the fjord. The results imply that benthic foraminiferal Ba/Ca in the coastal environment responds

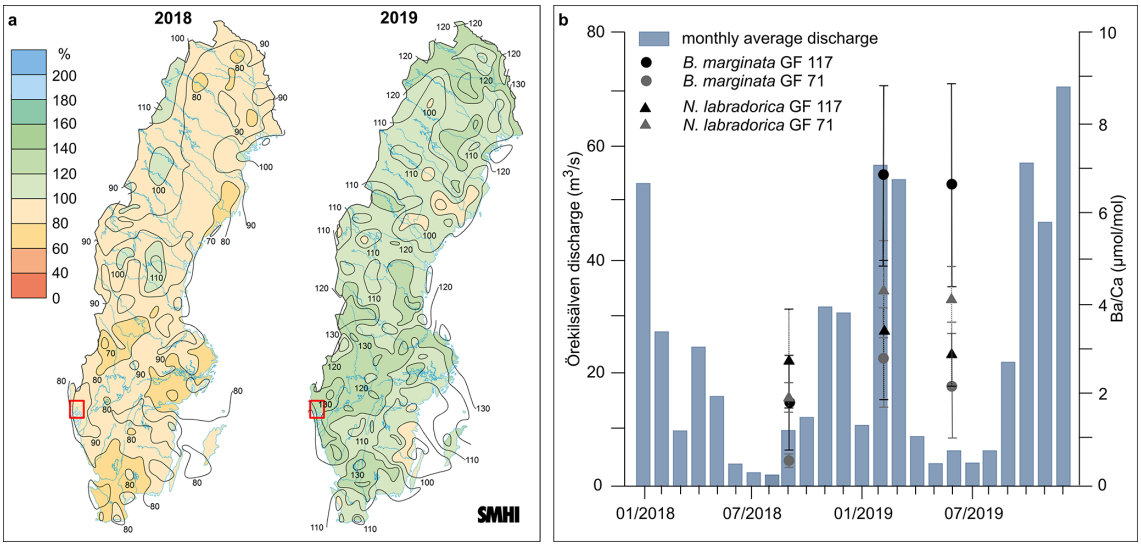

Figure 2. **(a)** Maps of Sweden showing annual average runoff in 2018 and 2019 compared to reference period 1961–1990 (SMHI), with study area marked by red rectangle. **(b)** Average monthly river discharge of Örekilsälven across 2018 and 2019 with median Ba/Ca with MAD per investigated species (n-chambers) and site indicated.

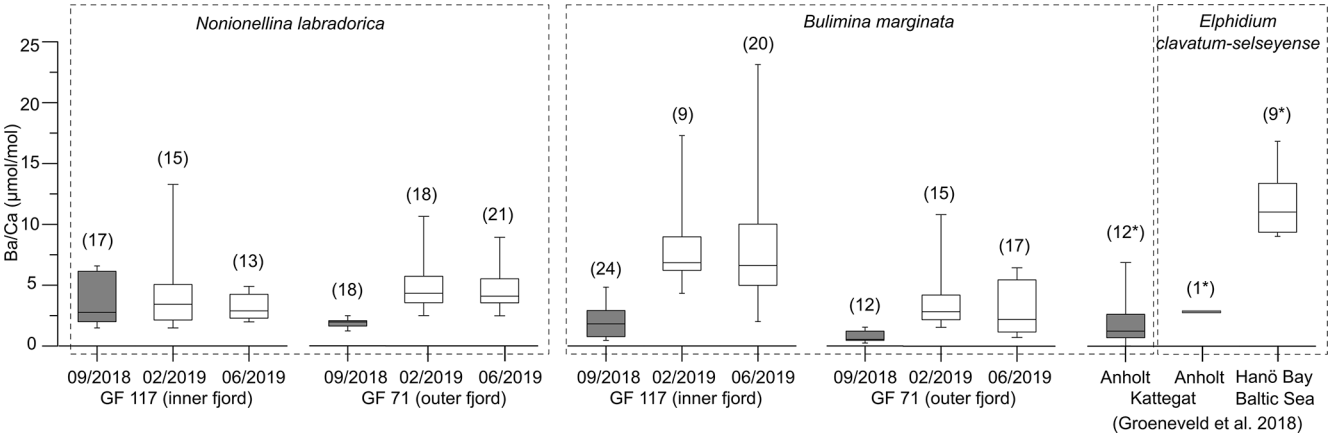

Figure 3. Box and whisker plots of benthic foraminiferal Ba/Ca from Gullmar Fjord (this study), Anholt (Kattegat) and Hanö Bay (Baltic Sea) (Groeneveld et al., 2018). Grey boxes represent samples from conditions without direct influence of terrestrial Ba addition, white boxes terrestrial-influenced samples. Number of analyzed specimens (for LA ICP-MS analyses) or bulk samples (of > 8 specimens each, ICP-OES analyses, marked by *) given in brackets. Note that Ba/Ca is derived from different species (marked by dashed rectangles).

on short timescales to the prevailing hydrological conditions on the adjacent continent.

4.2 Sediment evidence for Ba cycling in Gullmar Fjord

Barium is incorporated into foraminiferal tests proportionally to ambient concentrations (e.g., de Nooijer et al., 2017). Hence, contrasting Ba^{2+} availability in the foraminifera's microenvironment is a prerequisite for the observed benthic Ba/Ca signals. For planktonic foraminifera it has been shown that Ba incorporation is temperature- and salinity-independent (e.g., Hönisch et al., 2011). As both parameters were stable in the fjord ($T = 6.7 \pm 0.2\,°C$, $S = 34.4 \pm 0.1$), an influence on benthic Ba/Ca can be excluded. Bottom waters stayed oxygenated, albeit over a large gradient (ambient $[O_2]$ during sampling = 70–217 µmol L^{-1}; Fig. S3), and $[O_2]$ shows no correlation to benthic Ba/Ca. This implies that Ba^{2+} concentrations close to the sediment–water interface must have changed between the sampling moments.

The expected difference in Ba^{2+} availability between 2018 and 2019, however, is not clearly supported by the Ba sediment profiles obtained during sampling (Fig. 4; based on GF 117). Sedimentary Ba contents range from 3.11–3.53 µmol g^{-1}, indicating a strong enrichment relative to sediments of the Skagerrak (ca. 0.41 µmol g^{-1} particulate Ba; Lepland et al., 2000), confirming a near-shore accumulation

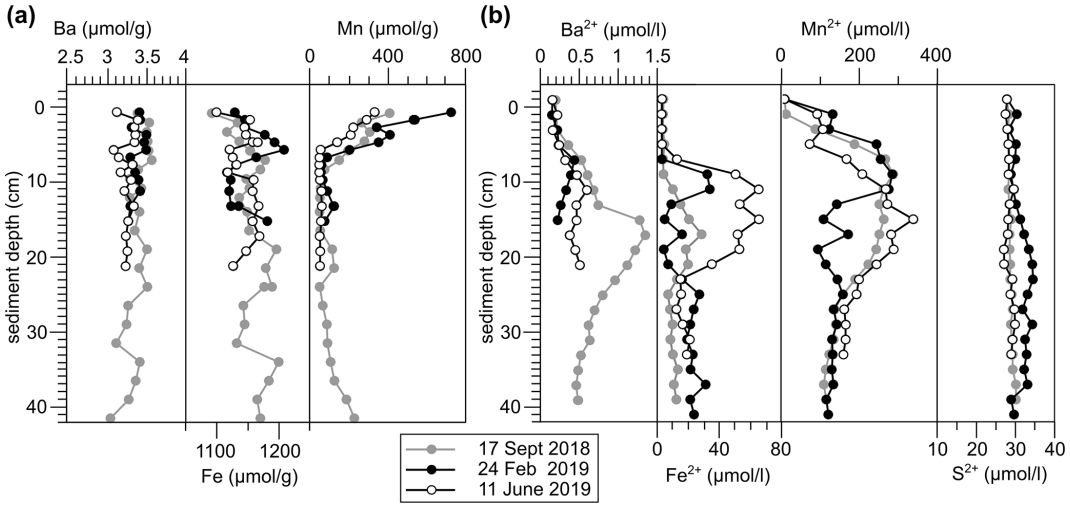

Figure 4. (a) Solid phase and **(b)** dissolved trace element profiles of site GF 117 at each sampling occasion.

due to terrigenous inputs. However, no significant changes were recorded in the surface sediment Ba concentration. Meanwhile, pore-water Ba profiles indicate diagenetic remobilization of Ba at depth in the sediment column. Values in excess of 1 µmol L^{-1} Ba^{2+} at 20 cm depth – distinctly higher than marine water column values (Kattegat [Ba] = 0.02–0.06 µmol L^{-1}, Groeneveld et al., 2018; global open ocean surface [Ba] = 0.04–0.05 µmol L^{-1}, Hsieh and Henderson, 2017) – support the concept of Ba release into pore waters fueling potential uptake into benthic foraminifera. However, the pore-water profiles also do not show significant changes between sampling years and most of the enrichment of Ba^{2+} in pore waters is observed deeper in the sediment column.

To explain the observed changes in foraminiferal Ba/Ca between 2018 and 2019 in the absence of whole-core sediment or pore-water geochemical evidence, we infer that rapid sub-annual processes at the sediment–water interface must be responsible. With sedimentation rates at the study sites being 0.7–0.9 cm yr^{-1} (Filipsson and Nordberg, 2004), only millimeters of new sediment material are expected to accumulate between the sampling occasions. Sub-annual changes in reactive Ba supply within this material, however, may dictate pore-water Ba release close to the sediment–water interface and uptake into benthic foraminifera. Such changes are unlikely to be captured in the pore-water profiles obtained at 2 cm resolution on the three sampling occasions. We infer therefore that during wet years such as 2019, reactive Ba is transported into the fjord in short-timescale pulses directed by continental rainfall and riverine discharge events, resulting in transient high fluxes of reactive Ba, which can be recorded by benthic foraminiferal Ba/Ca. Such temporally restricted fluxes may also explain the high relative standard deviation of Ba/Ca (in *n*-chambers of *B. marginata* = 46 %–71 %; *N. labradorica* = 17 %–69 %). While chamber precipitation in foraminifera is generally completed within a few hours (e.g., de Nooijer et al., 2009), population signals represent cumulative seasonal trends in terrestrial Ba input and benthic availability. In the following we explore potential sources of reactive Ba.

4.2.1 Potential sources of short-timescale changes in Ba/Ca: biogenic barite cycling

In marine environments Ba can be associated with various particulate phases, including detrital or "biogenic" barite ($BaSO_4$), and adsorbed to organic matter, carbonates, or metal oxides (e.g., Coffey et al., 1997; Dehairs et al., 1980; McManus et al., 1998). Of these, biogenic barite is the most commonly studied and therefore we must consider the potential of biogenic barite cycling to influence the observed signals in foraminiferal Ba/Ca.

In open-ocean settings primary productivity acts as the main facilitator of downward Ba transport: dissolved Ba is adsorbed or bound to primary producers and forms biogenic barite upon organic matter degradation in the water column (e.g., Dehairs et al., 1980; Martinez-Ruiz et al., 2019). Thereby, a Ba–productivity relationship develops that is frequently used to infer paleo-productivity changes from benthic foraminiferal Ba/Ca (e.g., Mojtahid et al., 2019; Ní Fhlaithearta et al., 2010). For example, shifts from low to high paleo-productivity periods reflect in benthic Ba/Ca increases by 2–3 times in the Mediterranean (before and during sapropel S1; Mojtahid et al., 2019; Ní Fhlaithearta et al., 2010) and < 1.5 in the Bahama Banks and Caribbean Sea (Last Glacial Maximum to deglaciation; Hall and Chan, 2004). However, this relationship is a function of water depth due to barite crystal growth rates and settling rates and cannot be reliably extended to shallow-water deposits as studied here (< 1000 m water depth; e.g., Von Breymann et al., 1992). Still, episodic removal of Ba^{2+} by barite formation in association with phytoplankton blooms is known from estuaries,

although typically showing rapid Ba regeneration with riverine discharge surges (e.g., Stecher and Kogut, 1999).

A theoretical mechanism for short-timescale release of Ba from biogenic barite in sediments is variable pore-water sulfate undersaturation (e.g., McManus et al., 1998). However, no evidence for this mechanism is observed in the fjord. Pore-water total S concentrations, primarily reflecting sulfate, are stable throughout the sediment column (Fig. 4b). Organo-clastic sulfate reduction (e.g., McManus et al., 1998) is primarily activated once more energetically beneficial electron acceptors are consumed (oxygen, nitrogen, manganese (Mn), iron (Fe); e.g., Froelich et al., 1979). In the sediments of GF the anaerobic reduction of Mn and Fe (oxyhydr)oxides (hereafter referred to as Mn or Fe oxides) dominates, as evidenced by pore-water Mn and Fe enrichments (down to ca. 12.5–25 cm depth; Fig. 4b). The fjord's high sedimentary Mn content makes sulfate reduction and diagenetic Ba^{2+} release within the habitat of benthic foraminifera generally unlikely (e.g., Vandieken et al., 2012). Hence, both biogenic and detrital barite can be considered as unreactive in this setting.

4.2.2 Ba and metal oxide cycling

In transition zones between fluvial and marine environments, such as GF, estuarine mixing behavior modulates Ba addition from the continents through the desorption of Ba^{2+} from suspended matter of fluvial origin (terrestrial aluminosilicates and other detrital material) by cation exchange at low to medium salinities (e.g., Coffey et al., 1997; Hanor and Chan, 1977). However, Ba may then become associated with Fe and Mn oxides (e.g., Coffey et al., 1997), due to the oxides' affinity for Ba and its chemical analogues (e.g., Balistrieri and Murray, 1986). This association potentially allows Ba to be sedimented in the near-shore environment, providing a mechanism for short-term changes in Ba supply to the seafloor.

An overall coupling of Ba to Mn (and Fe) cycling in the GF sediments is supported by the pore-water profiles showing coinciding pore-water maxima of these elements (Fig. 4) and positive inter-element correlations (Fig. S4). We propose that short-timescale pulses of Fe and Mn oxide sedimentation in association with discharge events also lead to rapid release of Ba into solution at the seafloor as oxides are utilized in the remineralization of fresh organic matter. Based on experimental estimates of Fe/Mn oxide particle settling velocity in the Baltic, oxides shuttle through the water column in the order of weeks, considering the water depths of the study sites (Glockzin et al., 2014). This constitutes a transport mechanism with a short temporal delay between surface Ba addition and foraminiferal incorporation at depth that is in line with the correlation of Ba/Ca to riverine fluxes strengthening with increasing time between sampling and river discharge period (see Sect. 4.1; Table S3).

The influence of Ba^{2+} liberated from recently accumulated Fe and Mn oxides appears to decrease below the water–sediment interface, where Ba^{2+} availability is dictated more by processes deeper in the sediment column. Barium is remobilized at depth in the sediment column during oxide reduction, as indicated by the upward diffusion of Ba^{2+} from below ca. 10 cm depth (Fig. 4b). This liberation of Ba^{2+} from Mn oxides appears to be constant, as well as negligible in magnitude compared to the terrigenous sedimentary Ba background signal, showing the dominance of non-reactive Ba in the system (Fig. 4a). Therefore, shallow-infaunal species such as *B. marginata* are expected to be exposed to greater variability in Ba^{2+} availability than deep infaunal species.

4.3 Proxy potential of *N. labradorica* and *B. marginata*

Ba/Ca of *N. labradorica* and *B. marginata* are significantly different for most seasons at each site (Table S4; Welch ANOVA). Partly, this may be an effect of species-specific differences in trace element incorporation, which has been documented for several taxa of foraminifera including *Bulimina* and *Nonionellina* (e.g., Barras et al., 2018; de Nooijer et al., 2017; Koho et al., 2017).

While *B. marginata*'s Ba/Ca reliably records fluctuations in terrestrial-derived Ba input, *N. labradorica* shows seasonal shifts in Ba/Ca only in the outer-fjord site. Against expectation, Ba/Ca of the inner-fjord site does not deviate substantially from values recorded during the drought period in 2018 in *N. labradorica*. This might be connected to a deeper effective living depth in this site, exposing the specimens to a constant, low-level supply of Ba^{2+} (as discussed in Sect. 4.2.2). Factors determining migration and distribution of this species comprise food supply and the bottom-water oxygenation regime (e.g., Alve and Bernhard, 1995), which conceivably could vary between the inner and outer fjord. *Nonionellina labradorica* was less abundant in the inner fjord. Generally, its abundance has been decreasing within GF since the early 1980s, likely driven by the increase in periods of bottom-water hypoxia ($[O_2] < 64\,\mu mol\,L^{-1}$) (e.g., Filipsson and Nordberg, 2004). This potential sensitivity of *N. labradorica*'s Ba/Ca signal to factors other than terrestrial input-driven Ba variability should be considered in proxy interpretations. Oppositely, *B. marginata* is particularly promising as a proxy for riverine discharge.

Incorporation of trace elements, including Ba^{2+}, is further known to be a function of ontogeny in some taxa, as calcification rates typically decrease and control of element partitioning increases over the growth of tests (e.g., de Nooijer et al., 2017). Analyses across successive chambers of *B. marginata* and *N. labradorica* do show significant differences between chambers for some samples (Mann–Whitney test, Table S5). Particularly the proloculus area of *B. marginata* exhibits almost consistently higher Ba/Ca ratios than later chambers (i.e., n, $n-1$, $n-2$; Fig. S1). Because the strength and direction of the inter-chamber correlations vary (Spearman rank correlation, Table S5) we infer a combined influence of on-

togeny and seasonal differences in pore-water [Ba] imprinting in successive chambers. As the sharp trend across the studied years is seen both in most recently formed chambers (n) and prior-formed chambers ($n-1$, $n-2$; p for *B. marginata*; Fig. S1), environmental changes appear to overprint ontogenetic effects on Ba/Ca at least across strong hydroclimatic gradients as experienced between 2018 and 2019.

5 Implications for applications of benthic Ba/Ca as paleo-river discharge and drought proxy

Our study highlights the potential of benthic foraminiferal Ba/Ca as indicator of drought and river discharge conditions in near-continent records, based on signals of living foraminifera populations. We demonstrate that the input of terrestrial Ba through riverine discharge and runoff is the dominant control on surface sediment Ba availability and foraminiferal Ba/Ca, in the investigated coastal region. As shallow-infaunal foraminifera (e.g., *B. marginata*) show a stronger response in Ba/Ca to continental hydroclimatic conditions, we deduce that their micro-habitat exposes them to higher Ba^{2+} variability from terrestrial sources, and therefore that these species may be more suitable as recorders of drought. The rapid cycling of bioavailable Ba at or close to the water–sediment interface appears to be modulated by the sedimentation and dissolution of Fe–Mn oxide carrier phases on short timescales. Therefore, we caution that a specific set of conditions may be required for the proxy to faithfully record hydroclimatic conditions. Most importantly, GF is characterized by high rates of Fe and Mn oxide accumulation under a generally oxic water column, which favors a strong role of dissimilatory oxide reduction in diagenesis and therefore enhanced oxide-mediated Ba cycling. Other systems with lower oxide fluxes or persistent anoxic conditions may not be suitable to record Ba/Ca signals of hydrodynamic changes.

In our data the variations in Ba/Ca are foremost explained by changes in physico-chemical parameters of the ambient environment during test precipitation but seem to be partly controlled by species-specific vital effects. While the seasonal trend in Ba/Ca across opposing river discharge conditions is significant even when pooling the two investigated taxa, we highlight that monospecific analyses are preferable. The data set suggests that ontogenetic trends in Ba incorporation of the studied species are probable. Nevertheless, as all investigated chambers show comparable trends in relation to continental hydroclimate conditions, at least on annual timescales, bulk trace-elemental analyses (of specimens of restricted test sizes) are likely sufficient for Ba/Ca proxy applications in paleo-studies. High-temporal-resolution interpretation of hydrodynamic changes in paleo-applications (e.g., sub-annual timescales) should be considered with caution unless uncertainties regarding the duration of Ba downward transport in the water column and lag between Ba input and foraminiferal incorporation can be resolved. Further, the sensitivity of the technique to more subtle changes than experienced between the extreme and contrasting weather conditions during 2018 and 2019 remains to be determined.

Further studies considering the interplay of riverine discharge, open-ocean water exchange, vertical and horizontal Ba transport, and hinterland precipitation are needed to assess the ability of the proxy to reconstruct river discharge quantitatively.

Data availability. The foraminiferal trace element data generated during this study are stored at the Swedish National Data Service (SND) under Brinkmann (2022).

Supplement. The supplement related to this article is available online at: https://doi.org/10.5194/bg-19-2523-2022-supplement.

Author contributions. The concept was developed by IB and HLF. IB, TJ, KMP, MS, and HLF participated in the sampling campaigns. IB, TJ, TN, and KMP performed the measurements. CB, TJ, and TN validated the data. IB analyzed the data and prepared the manuscript draft. All co-authors reviewed and edited the manuscript. HLF administered the project, provided resources, and supervised.

Competing interests. The contact author has declared that neither they nor their co-authors have any competing interests.

Disclaimer. Publisher's note: Copernicus Publications remains neutral with regard to jurisdictional claims in published maps and institutional affiliations.

Acknowledgements. The authors thank the captain and crew of the RV *Oscar von Sydow* and RV *Skagerak* for technical assistance. We thank Sami Jokinen and Hanna Nilsson for their help during the cruises. We acknowledge the staff of the Kristineberg Marine Research Station for their support during the field campaigns. Further, the hydrographic data used in this project are from SMHI's database, including SHARK. The SHARK data collection is organized by the Swedish environmental monitoring program and funded by the Swedish Agency for Marine and Water Management (SwAM). Finally, we thank the editor and the two anonymous referees for their feedback.

Financial support. This research has been supported by the Vetenskapsrådet (grant no. 2017-04190), the Kungliga Fysiografiska Sällskapet i Lund (grant no. –), the Academy of Finland (grant nos. 317684 and 319956), and the Crafoordska Stiftelsen (grant no. –).

Review statement. This paper was edited by Tyler Cyronak and reviewed by two anonymous referees.

References

Alve, E. and Bernhard, J. M.: Vertical migratory response of benthic foraminifera to controlled oxygen concentrations in an experimental mesocosm, Mar. Ecol. Prog. Ser., 116, 137–151, 1995.

Arneborg, L.: Turnover times for the water above sill level in Gullmar Fjord, Cont. Shelf Res., 24, 443–460, https://doi.org/10.1016/j.csr.2003.12.005, 2004.

Bahr, A., Schönfeld, J., Hoffmann, J., Voigt, S., Aurahs, R., Kucera, M., Flögel, S., Jentzen, A., and Gerdes, A.: Comparison of Ba/Ca and δ^{18}O as freshwater proxies: A multi-species core-top study on planktonic foraminifera from the vicinity of the Orinoco River mouth, Earth Planet Sc. Lett., 383, 45–57, https://doi.org/10.1016/j.epsl.2013.09.036, 2013.

Balistrieri, L. S. and Murray, J. W.: The surface chemistry of sediments from the Panama Basin: The influence of Mn oxides on metal adsorption, Geochim. Cosmochim. Ac., 50, 2235–2243, https://doi.org/10.1016/0016-7037(86)90078-5, 1986.

Barras, C., Aurélia, M., Pia, N. M., Edouard, M., Jassin, P., Carole, L., Filipsson, H. L., and Frans, J.: Experimental calibration of manganese incorporation in foraminiferal calcite, Geochim. Cosmochim. Ac., 237, 49–64, https://doi.org/10.1016/j.gca.2018.06.009, 2018.

Bastos, A., Fu, Z., Ciais, P., Friedlingstein, P., Sitch, S., Pongratz, J., Weber, U., Reichstein, M., Anthoni, P., Arneth, A., Haverd, V., Jain, A., Joetzjer, E., Knauer, J., Lienert, S., Loughran, T., McGuire, P. C., Obermeier, W., Padrón, R. S., Shi, H., Tian, H., Viovy, N., and Zaehle, S.: Impacts of extreme summers on European ecosystems: a comparative analysis of 2003, 2010 and 2018, Philos. T. Roy. Soc. B, 375, 20190507, https://doi.org/10.1098/rstb.2019.0507, 2020a.

Bastos, A., Ciais, P., Friedlingstein, P., Sitch, S., Pongratz, J., Fan, L., Wigneron, J. P., Weber, U., Reichstein, M., Fu, Z., Anthoni, P., Arneth, A., Haverd, V., Jain, A. K., Joetzjer, E., Knauer, J., Lienert, S., Loughran, T., McGuire, P. C., Tian, H., Viovy, N., and Zaehle, S.: Direct and seasonal legacy effects of the 2018 heat wave and drought on European ecosystem productivity, Sci. Adv., 6, eaba2724, https://doi.org/10.1126/sciadv.aba2724, 2020b.

Bernhard, J. M., Ostermann, D. R., Williams, D. S., and Blanks, J. K.: Comparison of two methods to identify live benthic foraminifera: A test between Rose Bengal and CellTracker Green with implications for stable isotope paleoreconstructions, Paleoceanography, 21, PA4210, https://doi.org/10.1029/2006PA001290, 2006.

Burdige, D. J.: Geochemistry of marine sediments, Princeton University Press, Princeton, NJ, USA, https://doi.org/10.2307/j.ctv131bw7s, 2006.

Brinkmann, I.: Trace-elemental data (Ba/Ca) of benthic foraminifers from core-top sediments of Gullmar Fjord, Swedish West coast, Swedish National Data Service [data set], 1, https://doi.org/10.5878/eb67-9v72, 2022.

Coffey, M., Dehairs, F., Collette, O., Luther, G., Church, T., and Jickells, T.: The behaviour of dissolved Barium in estuaries, Estuar. Coast Shelf Sci., 45, 113–121, https://doi.org/10.1006/ecss.1996.0157, 1997

Cook, B. I., Mankin, J. S., Marvel, K., Williams, A. P., Smerdon, J. E., and Anchukaitis, K. J.: Twenty-first century drought projections in the CMIP6 forcing scenarios, Earth's Future, 8, e2019EF001461, https://doi.org/10.1029/2019ef001461, 2020.

de Nooijer, L. J., Toyofuku, T., and Kitazato, H.: Foraminifera promote calcification by elevating their intracellular pH, P. Natl. Acad. Sci. USA, 106, 15374–15378, https://doi.org/10.1073/pnas.0904306106, 2009.

de Nooijer, L. J., Brombacher, A., Mewes, A., Langer, G., Nehrke, G., Bijma, J., and Reichart, G.-J.: Ba incorporation in benthic foraminifera, Biogeosciences, 14, 3387–3400, https://doi.org/10.5194/bg-14-3387-2017, 2017.

Dehairs, F., Chesselet, R., and Jedwab, J.: Discrete suspended particles of barite and the barium cycle in the open ocean, Earth Planet. Sc. Lett., 49, 528–550, https://doi.org/10.1016/0012-821X(80)90094-1, 1980.

Dunn, R. J. H., Stanitski, D. M., Gobron, N., and Willett, K. M.: Global Climate, in: State of the Climate in 2019, edited by: Blunden, J. and Arndt, D. S., B. Am. Meteorol. Soc., 101, 9–128, https://doi.org/10.1175/BAMS-D-20-0104.1, 2020.

Eggins, S. M., Rudnick, R. L., and McDonough, W. F.: The composition of peridotites and their minerals: a laser-ablation ICP–MS study, Earth Planet. Sc. Lett., 154, 53–71, https://doi.org/10.1016/S0012-821X(97)00195-7, 1998.

Erez, J.: The source of ions for biomineralization in foraminifera and their implications for paleoceanographic proxies, Rev. Mineral. Geochem., 54, 115–149, https://doi.org/10.2113/0540115, 2003.

Filipsson, H. L. and Nordberg, K.: Climate variations, an overlooked factor influencing the recent marine environment, An example from Gullmar Fjord, Sweden, illustrated by benthic foraminifera and hydrographic data, Estuaries, 27, 867–881, https://doi.org/10.1007/BF02912048, 2004.

Froelich, P. N., Klinkhammer, G., Bender, M. L., Luedtke, N., Heath, G. R., Cullen, D., Dauphin, P., Hammond, D., Hartman, B., and Maynard, V.: Early oxidation of organic matter in pelagic sediments of the eastern equatorial Atlantic: suboxic diagenesis, Geochim. Cosmochim. Ac., 43, 1075–1090, https://doi.org/10.1016/0016-7037(79)90095-4, 1979.

GeoReM: Geological and Environmental Reference Material: http://georem.mpch-mainz.gwdg.de, last access: 30 April 2021.

Glockzin, M., Pollehne, F., and Dellwig, O.: Stationary sinking velocity of authigenic manganese oxides at pelagic redoxclines, Mar. Chem., 160, 67–74, https://doi.org/10.1016/j.marchem.2014.01.008, 2014.

Groeneveld, J., Filipsson, H. L., Austin, W. E., Darling, K., McCarthy, D., Krupinski, N. B. Q., Bird, C., and Schweizer, M.: Assessing proxy signatures of temperature, salinity, and hypoxia in the Baltic Sea through foraminifera-based geochemistry and faunal assemblages, J. Micropalaentol., 37, 403–429, https://doi.org/10.5194/jm-37-403-2018, 2018.

Gustafsson, M. and Nordberg, K.: Living (stained) benthic foraminiferal response to primary production and hydrography in the deepest part of the Gullmar Fjord, Swedish West Coast, with comparisons to Höglund's 1927 material, J. Foraminiferal. Res., 31, 2–11, https://doi.org/10.2113/0310002, 2001.

Hall, J. M. and Chan, L. H.: Ba/Ca in benthic foraminifera: Thermocline and middepth circulation in the North Atlantic during the last glaciation, Paleoceanography, 19, PA4018, https://doi.org/10.1029/2004PA001028, 2004.

Hammer, O., Harper, D. A. T., and Ryan, P. D.: PAST: Paleontological statistics software package for education and data analysis, Palaeontol. Electron., 4, 9 pp., http://palaeo-electronica.org/2001_1/past/issue1_01.htm (last access: 30 April 2021), 2001.

Hanor, J. S. and Chan, L. H.: Non-conservative behavior of barium during mixing of Mississippi River and Gulf of Mexico waters, Earth Planet. Sc. Lett., 37, 242–250, https://doi.org/10.1016/0012-821X(77)90169-8, 1977.

Hönisch, B., Allen, K. A., Russell, A. D., Eggins, S. M., Bijma, J., Spero, H. J., Lea, D. W., and Yu, J.: Planktic foraminifers as recorders of seawater Ba/Ca, Mar. Micropaleontol., 79, 52–57, https://doi.org/10.1016/j.marmicro.2011.01.003, 2011.

Howe, J. A., Austin, W. E., Forwick, M., Paetzel, M., Harland, R., and Cage, A. G.: Fjord systems and archives: a review, Geol. Soc. Spec. Publ., 344, 5–15, https://doi.org/10.1144/SP344.2, 2010.

Hsieh, Y.-T. and Henderson, G. M.: Barium stable isotopes in the global ocean: Tracer of Ba inputs and utilization, Earth Planet. Sc. Lett., 473, 269–278, https://doi.org/10.1016/j.epsl.2017.06.024, 2017.

Jochum, K. P., Nohl, U., Herwig, K., Lammel, E., Stoll, B., and Hofmann, A. W.: GeoReM: A new geochemical database for reference materials and isotopic standards, Geostand. Geoanal. Res., 29, 333–338, https://doi.org/10.1111/j.1751-908X.2005.tb00904.x, 2005.

Jochum, K. P., Scholz, D., Stoll, B., Weis, U., Wilson, S. A., Yang, Q., Schwalb, A., Börner, N., Jacob, D. E., and Andreae, M. O.: Accurate trace element analysis of speleothems and biogenic calcium carbonates by LA-ICP-MS, Chem. Geol., 318, 31–44, https://doi.org/10.1016/j.chemgeo.2012.05.009, 2012.

Jokinen, S. A., Koho, K., Virtasalo, J. J., and Jilbert, T.: Depth and intensity of the sulfate-methane transition zone control sedimentary molybdenum and uranium sequestration in a eutrophic low-salinity setting, Appl. Geochem., 122, 104767, https://doi.org/10.1016/j.apgeochem.2020.104767, 2020.

Koho, K. A., de Nooijer, L. J., Fontanier, C., Toyofuku, T., Oguri, K., Kitazato, H., and Reichart, G.-J.: Benthic foraminiferal Mn/Ca ratios reflect microhabitat preferences, Biogeosciences, 14, 3067–3082, https://doi.org/10.5194/bg-14-3067-2017, 2017.

Kornhuber, K., Osprey, S., Coumou, D., Petri, S., Petoukhov, V., Rahmstorf, S., and Gray, L.: Extreme weather events in early summer 2018 connected by a recurrent hemispheric wave-7 pattern, Environ. Res. Lett., 14, 054002, https://doi.org/10.1088/1748-9326/ab13bf, 2019.

Lepland, A., Sæther, O., and Thorsnes, T.: Accumulation of barium in recent Skagerrak sediments: sources and distribution controls, Mar. Geol., 163, 13–26, https://doi.org/10.1016/S0025-3227(99)00104-8, 2000.

Martinez-Ruiz, F., Paytan, A., Gonzalez-Muñoz, M. T., Jroundi, F., Abad, M. M., Lam, P. J., Bishop, J. K. B., Horner, T. J., Morton, P. L., and Kastner, M.: Barite formation in the ocean: Origin of amorphous and crystalline precipitates, Chem. Geol., 511, 441–451, https://doi.org/10.1016/j.chemgeo.2018.09.011, 2019.

Mashiotta, T. A., Lea, D. W., and Spero, H. J.: Glacial–interglacial changes in subantarctic sea surface temperature and δ^{18}O-water using foraminiferal Mg, Earth Planet. Sc. Lett., 170, 417–432, https://doi.org/10.1016/S0012-821X(99)00116-8, 1999.

McManus, J., Berelson, W. M., Klinkhammer, G. P., Johnson, K. S., Coale, K. H., Anderson, R. F., Kumar, N., Burdige, D. J., Hammond, D. E., Brumsack, H. J., McCorkle, D. C., and Rushdi, A.: Geochemistry of barium in marine sediments: implications for its use as a paleoproxy, Geochim. Cosmochim. Ac., 62, 3453–3473, https://doi.org/10.1016/S0016-7037(98)00248-8, 1998.

Mojtahid, M., Hennekam, R., De Nooijer, L., Reichart, G.-J., Jorissen, F., Boer, W., Le Houedec, S., and De Lange, G. J.: Evaluation and application of foraminiferal element/calcium ratios: Assessing riverine fluxes and environmental conditions during sapropel S1 in the Southeastern Mediterranean, Mar. Micropaleontol., 153, 101783, https://doi.org/10.1016/j.marmicro.2019.101783, 2019.

Murray, J.: Ecology and Applications of Benthic Foraminifera, Cambridge University Press, Cambridge, UK, ISBN 9780521828390, 2006.

Ní Fhlaithearta, S., Reichart, G.-J., Jorissen, F. J., Fontanier, C., Rohling, E. J., Thomson, J., and De Lange, G. J.: Reconstructing the seafloor environment during sapropel formation using benthic foraminiferal trace metals, stable isotopes, and sediment composition, Paleoceanography, 25, PA4225, https://doi.org/10.1029/2009pa001869, 2010.

Ni, S., Krupinski, N. B. Q., Groeneveld, J., Fanget, A. S., Böttcher, M. E., Liu, B., Lipka, M., Knudsen, K. L., Naeraa, T., Seidenkrantz, M. S., and Filipsson, H. L.: Holocene hydrographic variations from the Baltic-North Sea transitional area (IODP site M0059), Paleoceanogr. Paleoclimatol., 35, e2019PA003722, https://doi.org/10.1029/2019pa003722, 2020.

Paton, C., Hellstrom, J., Paul, B., Woodhead, J., and Hergt, J.: Iolite: Freeware for the visualisation and processing of mass spectrometric data, J. Anal. At. Spectrom., 26, 2508–2518, https://doi.org/10.1039/C1JA10172B, 2011.

Paytan, A. and Griffith, E. M.: Marine barite: Recorder of variations in ocean export productivity, Deep-Sea Res. Pt. II, 54, 687–705, https://doi.org/10.1016/j.dsr2.2007.01.007, 2007.

Peters, W., Bastos, A., Ciais, P., and Vermeulen, A.: A historical, geographical and ecological perspective on the 2018 European summer drought, Philos. T. Roy. Soc. B, 375, 20190505, https://doi.org/10.1098/rstb.2019.0505, 2020.

Saha, N., Rodriguez-Ramirez, A., Nguyen, A. D., Clark, T. R., Zhao, J.-X., and Webb, G. E.: Seasonal to decadal scale influence of environmental drivers on Ba/Ca and Y/Ca in coral aragonite from the southern Great Barrier Reef, Sci. Total Environ., 639, 1099–1109, https://doi.org/10.1016/j.scitotenv.2018.05.156, 2018.

Stecher, H. A. and Kogut, M. B.: Rapid barium removal in the Delaware estuary, Geochim. Cosmochim. Ac., 63, 1003–1012, https://doi.org/10.1016/S0016-7037(98)00310-X, 1999.

Steiger, N. J., Smerdon, J. E., Cook, E. R., and Cook, B. I.: A reconstruction of global hydroclimate and dynamical variables over the Common Era, Sci. Data, 5, 180086, https://doi.org/10.1038/sdata.2018.86, 2018.

Sternberg, T.: Regional drought has a global impact, Nature, 472, 169–169, https://doi.org/10.1038/472169d, 2011.

SHARK: Svenskt HavsARKivs hydrographic database: https://sharkweb.smhi.se/hamta-data/, last access: 10 February 2021.

SMHI: Swedish Meteorological and Hydrological Institute's database [data set], https://www.smhi.se/, last access: 10 February.

Tallaksen, L. M. and Van Lanen, H. A. (Eds.): Hydrological drought: processes and estimation methods for streamflow and groundwater, Dev. Water Sci., Elsevier, Amsterdam, Netherlands, 48 pp., 2004.

Vandieken, V., Pester, M., Finke, N., Hyun, J.-H., Friedrich, M. W., Loy, A., and Thamdrup, B.: Three manganese oxide-rich marine sediments harbor similar communities of acetate-oxidizing manganese-reducing bacteria, ISME J., 6, 2078–2090, https://doi.org/10.1038/ismej.2012.41, 2012.

Vattenweb hydrological database: https://www.smhi.se/data/hydrologi/vattenwebb, last access: 10 February 2021.

Von Breymann, M. T., Emeis, K.-C., and Suess, E.: Water depth and diagenetic constraints on the use of barium as a palaeoproductivity indicator, Geol. Soc. Spec. Publ., 64, 273–284, https://doi.org/10.1144/gsl.Sp.1992.064.01.18, 1992.

Wit, J., Reichart, G.-J., Jung, S., and Kroon, D.: Approaches to unravel seasonality in sea surface temperatures using paired single-specimen foraminiferal δ^{18}O and Mg/Ca analyses, Paleoceanography, 25, PA4220, https://doi.org/10.1029/2009PA001857, 2010.

Wolgemuth, K. and Broecker, W. S.: Barium in sea water, Earth Planet. Sc. Lett., 8, 372–378, https://doi.org/10.1016/0012-821X(70)90110-X, 1970.